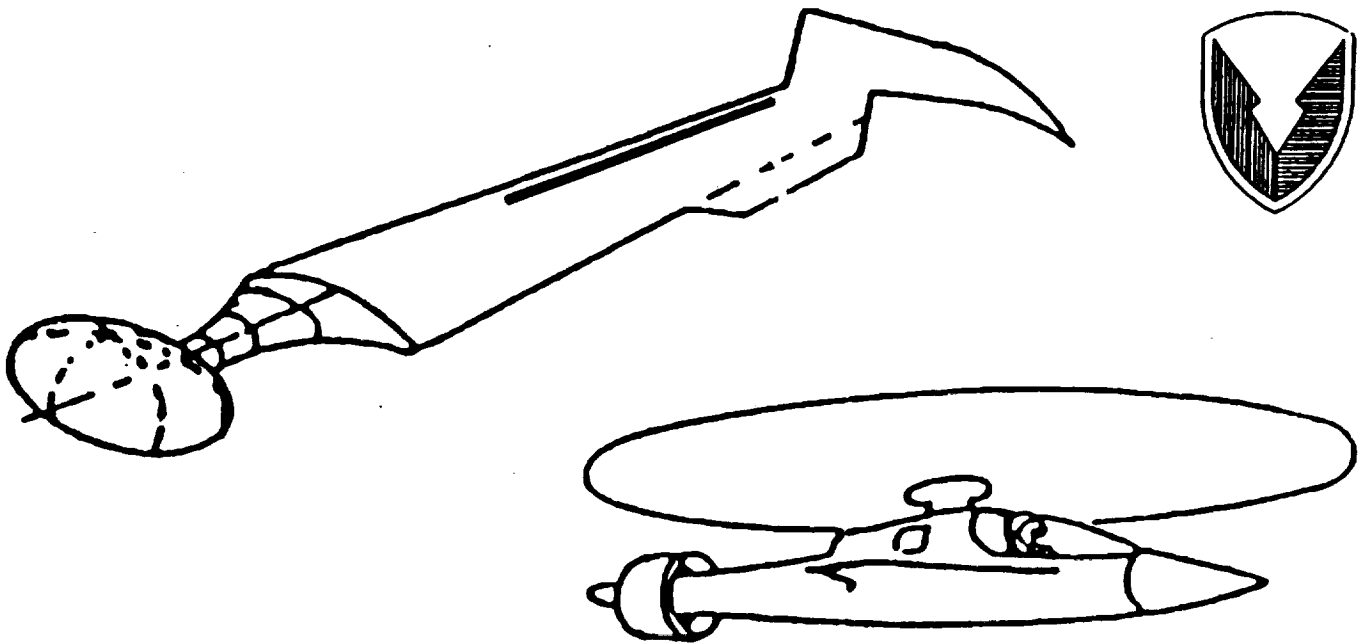


N94- 34986

THE QUEST FOR STALL-FREE DYNAMIC LIFT

by

C. Tung, K.W. McAlister, L.W. Carr,
E. Duque and R. Zinner



Army Aeroflightdynamics Directorate
Ames Research Center
Moffett Field, California

Presented at the Workshop On Physics Of Forced Unsteady Separation;
NASA-Ames Research Center; Moffett Field, California; April 17-19, 1990.



THE QUEST FOR STALL-FREE DYNAMIC LIFT

by

C. Tung, K.W. McAlister, L.W. Carr,
E. Duque and R. Zinner

INTRODUCTION

During the past decade, numerous major efforts have addressed the question of how to control or alleviate dynamic stall effects on helicopter rotors, but little concrete evidence of any significant reduction of the adverse characteristics of the dynamic stall phenomenon has been demonstrated. Nevertheless, it is important to remember that the control of dynamic stall is an achievable goal. Experiments performed at the US Army Aeroflight-dynamics Directorate more than a decade ago demonstrated that dynamic stall is not an unavoidable penalty of high amplitude motion, and that airfoils can indeed operate dynamically at angles far above the static-stall angle without necessarily forming a stall vortex. These experiments, one of them featuring a slat that was designed from static airfoil considerations, showed that unsteadiness can be a very beneficial factor in the development of high-lift devices for helicopter rotors.

The experience drawn from these early experiments is now being focused on a program for the alleviation of dynamic-stall effects on helicopter rotors. The purpose of this effort is to demonstrate that rotor stall can be controlled through an improved understanding of the unsteady effects on airfoil stall and to document the role of specific means that lead to stall alleviation in the 3-D unsteady environment of helicopter rotors in forward flight. The first concept to be addressed in this program will be a slatted airfoil. A 2D unsteady Navier-Stokes code has been modified to compute the flow around a two-element airfoil.

BACKGROUND

Dynamic stall continues to be a serious factor in modern helicopter design. The impulsive loads that are generated during helicopter airfoil stall limit high speed helicopter flight and reduce the maneuvering capability of the aircraft. The character of the dynamic stall phenomenon has been carefully studied (Refs. 1-3) and a significant body of knowledge has been acquired concerning the behavior of various airfoils during dynamic stall (Refs. 4-6). These studies have shown that deep stall is relatively insensitive to the airfoil profile; however, there are definite indications that dynamic stall inception is sensitive to the character of the boundary-layer (Ref. 3).

In order to better understand the significance of the boundary layer on the stall behavior, a variety of passive stall modifications were tested on an oscillating VR-7 airfoil (Ref. 7). In this study, a backward-facing step was installed in an attempt to control the progression of flow reversal on the airfoil and thus delay the formation of the stall vortex. Although several backward-facing step configurations were tested, no significant effect on the vortex development or the dynamic stall airloads was detected. Vortex generators were then installed at 20% chord to delay stall through boundary-layer re-energization. The vortex generators delayed the static stall significantly and even kept the boundary layer attached on the rearward portion of the airfoil under dynamic conditions. However, use of the vortex generators induced leading-edge stall in the dynamic environment and the loads were not measurably improved.

Finally, a leading-edge slat was installed in order to shift to the slat the rapid flow accelerations that normally occur near the leading edge of the basic airfoil and to re-energize the boundary layer on the main airfoil. A detailed diagram of this particular slat/airfoil combination is shown in Figure 1. This slat was found to postpone the dynamic stall to angles well above the range normally expected on helicopter airfoils, with virtually no drag penalty in the angle range associated with retreating blade aerodynamic conditions. A qualitative comparison of the slat/airfoil combination to that of the basic airfoil is presented in Figure 2. To approximate the full contribution of the slat/airfoil combination, the lift and moment curves were adjusted to match that of the basic airfoil at $\alpha = 15^\circ$. Figure 3 presents the lift and moment coefficients for the basic VR-7 airfoil for pitch oscillations of $\alpha = 15^\circ + 10^\circ \sin(\omega t)$ and for a range of frequencies. The dynamic

stall effects are quite evident. Figure 4 presents the same conditions for the slat/airfoil combination where it is clear that the dynamic stall vortex is no longer present. Figure 5 shows a comparison of the instantaneous pressure distributions for the basic airfoil and for the slat/airfoil combination at the same test conditions. Note the movement of the dynamic stall vortex along the chord of the basic airfoil and the complete absence of the vortex imprint in the slatted airfoil results.

APPROACH TO CONCEPT EVALUATION

The results in Reference 7 demonstrate the dramatic involvement that can be achieved by the use of a slat: the dynamic stall vortex is completely suppressed throughout the cycle of oscillation at the moderate frequencies that are compatible with helicopter forward-flight conditions. However, the slat/airfoil combination tested may not be the optimum shape nor even an acceptable configuration for a rotor application. Although the addition of the slat was effective in suppressing stall, the drag penalty is too large at the lower angles-of-attack (Fig. 6). A more acceptable design for the rotor would have to feature a retractable slat in order to avoid the high-drag penalty that would otherwise occur on the advancing side of the rotor disk. Encouraged by the success of the slat in suppressing the stall vortex, a new program called High Maneuverability and Agility Rotor and Control System (HIMARCS) has been initiated to study different techniques for increasing dynamic lift without stall. At the present time, the slat/airfoil combination is being reexamined in order to validate new CFD codes and to determine if the water tunnel can be used to qualitatively assess the performance of various high-lift concepts.

A general purpose code which solves the conservative thin-layer Navier-Stokes equations in generalized coordinates (Ref. 8) has been modified to handle the multi-element airfoil and includes an algebraic turbulence model (Ref. 9). Figure 7 compares the force and moment results for the basic VR-7 to the static results from an earlier wind tunnel experiment at $M_\infty = 0.3$ and $Re = 4.2 \times 10^6$ (Ref. 3). The computed lift coefficients show a reasonably good agreement with the test data. The moment coefficients also compare reasonably well at low angles-of-attack, but seriously under predict at high angles-of-attack. The drag coefficients are over predicted at low angles-of-attack, but are under predicted at higher angles-of-attack. This

over prediction of the drag at low angles-of-attack is expected since the computation assumed a fully turbulent boundary layer and in the experiment the boundary layer was allowed to undergo natural transition. Figure 8 compares the computed lift and drag coefficients for the basic and slatted VR-7 airfoil with the test results in Reference 7. Again the lift coefficients compare much better than the drag coefficients. Figure 9 shows the calculated Mach number and pressure coefficient contours for the slatted VR-7 airfoil at $\alpha = 15^\circ$. The enlarged views of these contours illustrate the ability of the code to model the interaction between the slat wake and the main-element boundary layer.

The slatted VR-7 airfoil will also be tested in the water-tunnel facility where total lift, drag and pitching moment measurements can be made. These results will be used to establish the scaling law between the comparatively low Reynolds number environment in the water tunnel and the higher Reynolds numbers attainable in the wind tunnel. The water tunnel results will also be used to complement the CFD efforts. A water-tunnel model of the VR-7 with slat has been constructed (Fig. 10) and a comparison between the experiment and the CFD calculations will be published in the near future (Ref. 10). Once greater confidence has been established in the CFD code as well as the use of the water tunnel for qualifying a candidate concept, a slotted airfoil will be designed. After the slot shape and position has been optimized, a set of slotted rotor blades will be constructed and the concept demonstrated under forward-flight conditions. The HIMARCS program will eventually address numerous high lift and control concepts as suggested in Figure 11.

REFERENCES

¹Carr, L.W.; McAlister, K.W. and McCroskey, W.J.: "Analysis of the Development of Dynamic Stall Based on Oscillating Airfoil Experiments." NASA TN D-8382, Jan. 1977.

²McCroskey, W.J.; McAlister, K.W.; Carr, L.W.; Pucci, S.L.; Lambert, O. and Indergand, R.F.: "Dynamic Stall on Advanced Airfoil Sections." J. American Helicopter Society, Vol. 26, No.3, July 1981, pp. 40-50.

³McCroskey, W.J.; McAlister, K.W.; Carr, L.W.; and Pucci, S.L.: "An Experimental Study of Dynamic Stall on Advanced airfoil Sections, Vol. 1,2,3." NASA TM-84245, July 1982.

⁴Ham, N.D. and Garelick, M.S.: "Dynamic Stall Considerations in Helicopter Rotors." J. of American Helicopter Society, Vol.13, No.2, April 1968, pp.49-55.

⁵Carta, F.O.; Commerford, G.L.; Carlson, R.G. and Blackwell, R.H.: "Investigation of Airfoil Dynamic Stall and its Influence on Helicopter Control Loads." USSAAMRDL TR 72-51, Sept. 1972.

⁶Liiva, J.: "Two-Dimensional Tests of Airfoils Oscillating Near Stall." J. of Aircraft, Vol. 6, No. 1, Jan. 1969 pp.46-51.

⁷Carr, L.W. and McAlister, K.W.: "The Effect of a Leading-Edge Slat on the Dynamic Stall of an Oscillating Airfoil." AIAA paper 83-2533, Oct. 1983.

⁸Steger, J.L.; Ying, S.X. and Schiff, L.N.: "A Partially Flux Split Algorithm for Numerical Simulations of Compressible Inviscid and Viscous Flow." Workshop on Computational Fluid Dynamics, Institute of Non-Linear Science, University of California, Davis, CA, 1986.

⁹Baldwin, B.S. and Lomax, H.: "Thin-layer Approximation and Algebraic Model for Separated Turbulent Flows." AIAA paper 78-257, Huntsville, Alabama, Jan. 1978.

¹⁰Duque, E.P.N.; Zinner, R.A. and McAlister, K.W.: "Static Stall Prediction for Single and Multi-Element Airfoils." to be published at ASME 1990 Winter Annual Meeting.

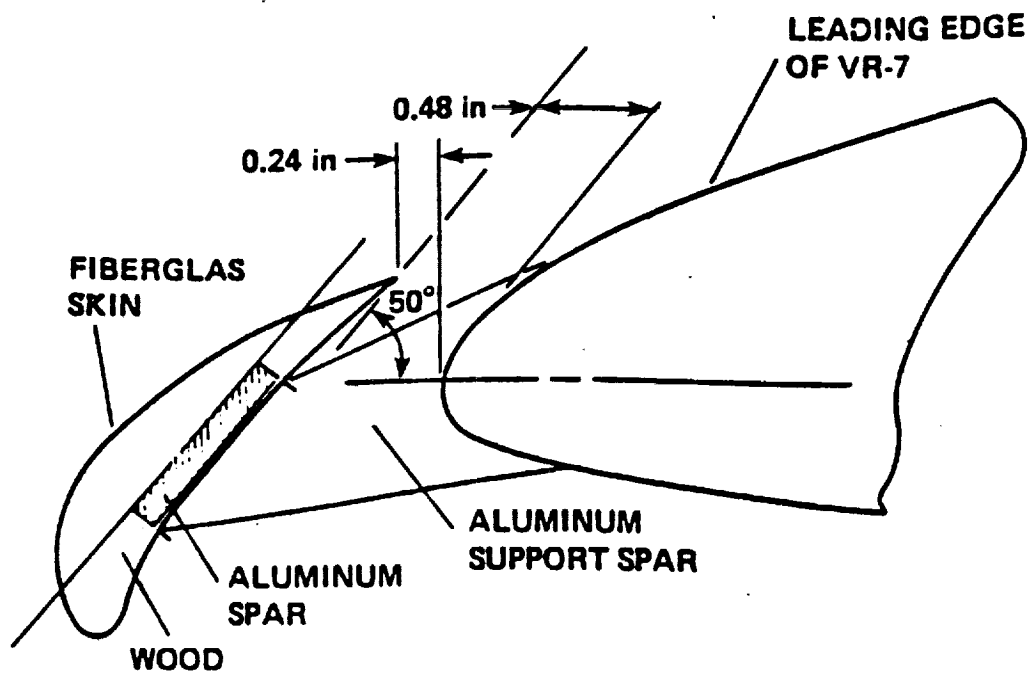


Figure 1.- Detailed sketch of VR-7 airfoil with slat.

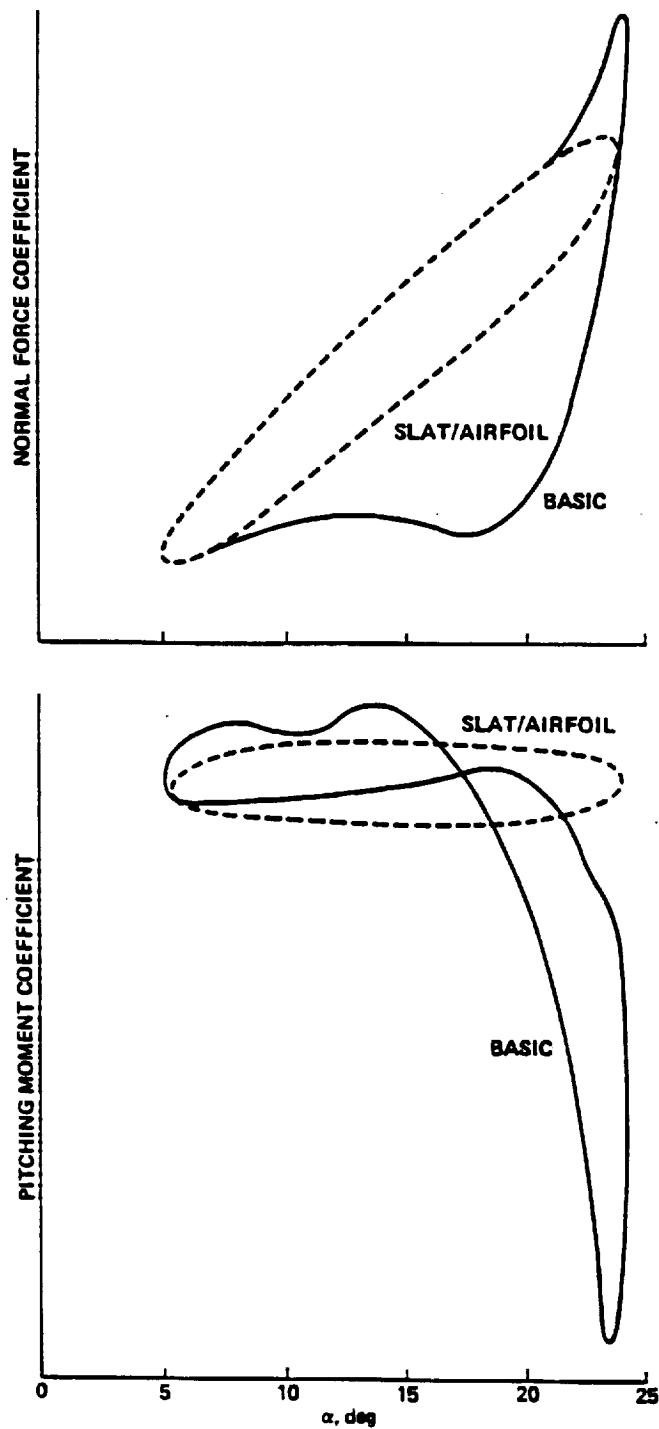


Figure 2.- Lift and moment measurements on the basic and slatted VR-7 airfoils at $k = 0.15$, $\alpha = 15^\circ + 10^\circ \sin \omega t$, $M_\infty = 0.185$ and $Re = 2.5 \times 10^6$.

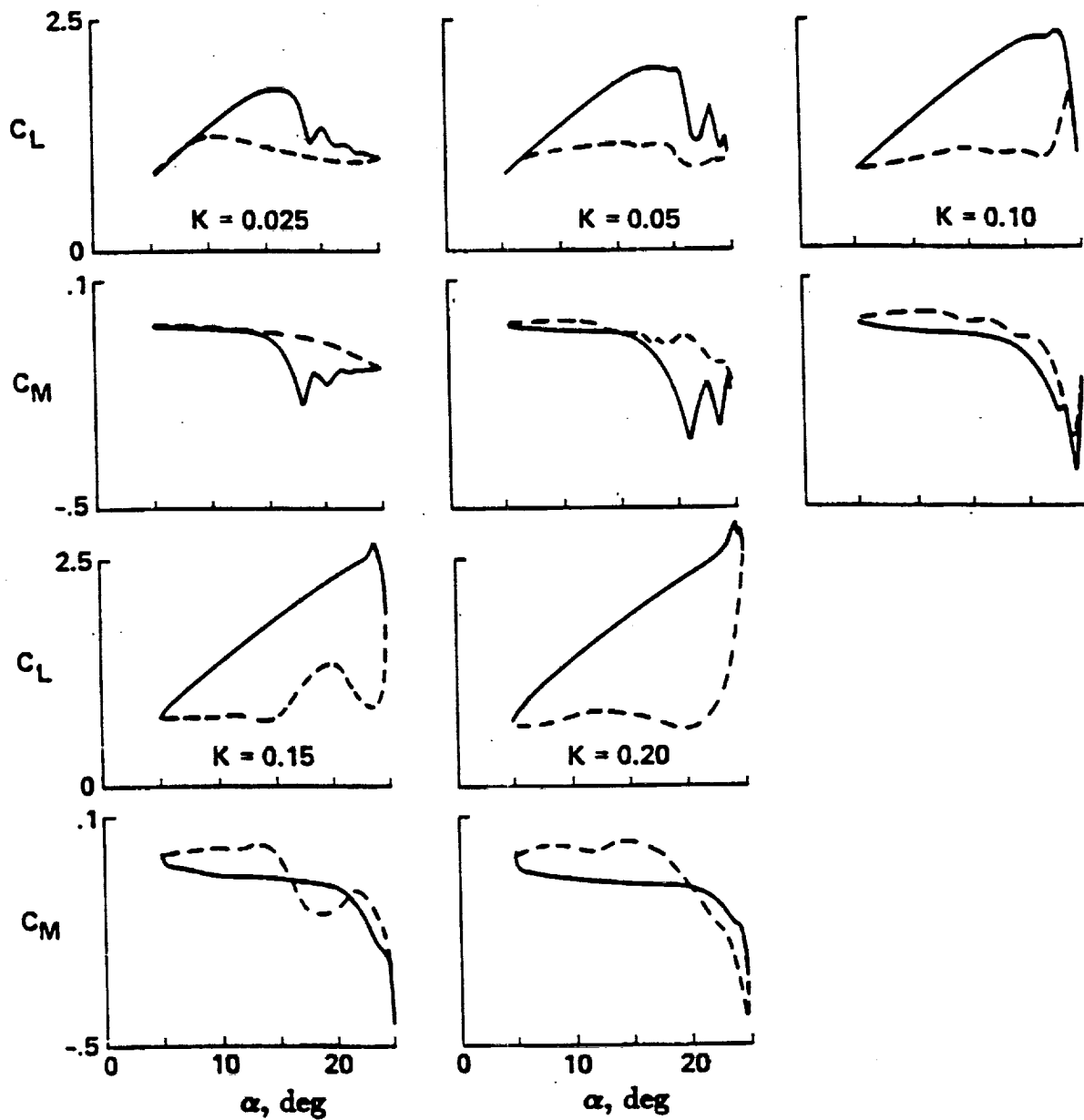


Figure 3.- Lift and moment coefficients for the basic VR-7 airfoil over a range of frequencies at $\alpha = 15^\circ + 10^\circ \sin \omega t$. Dashed lines indicate decreasing α .

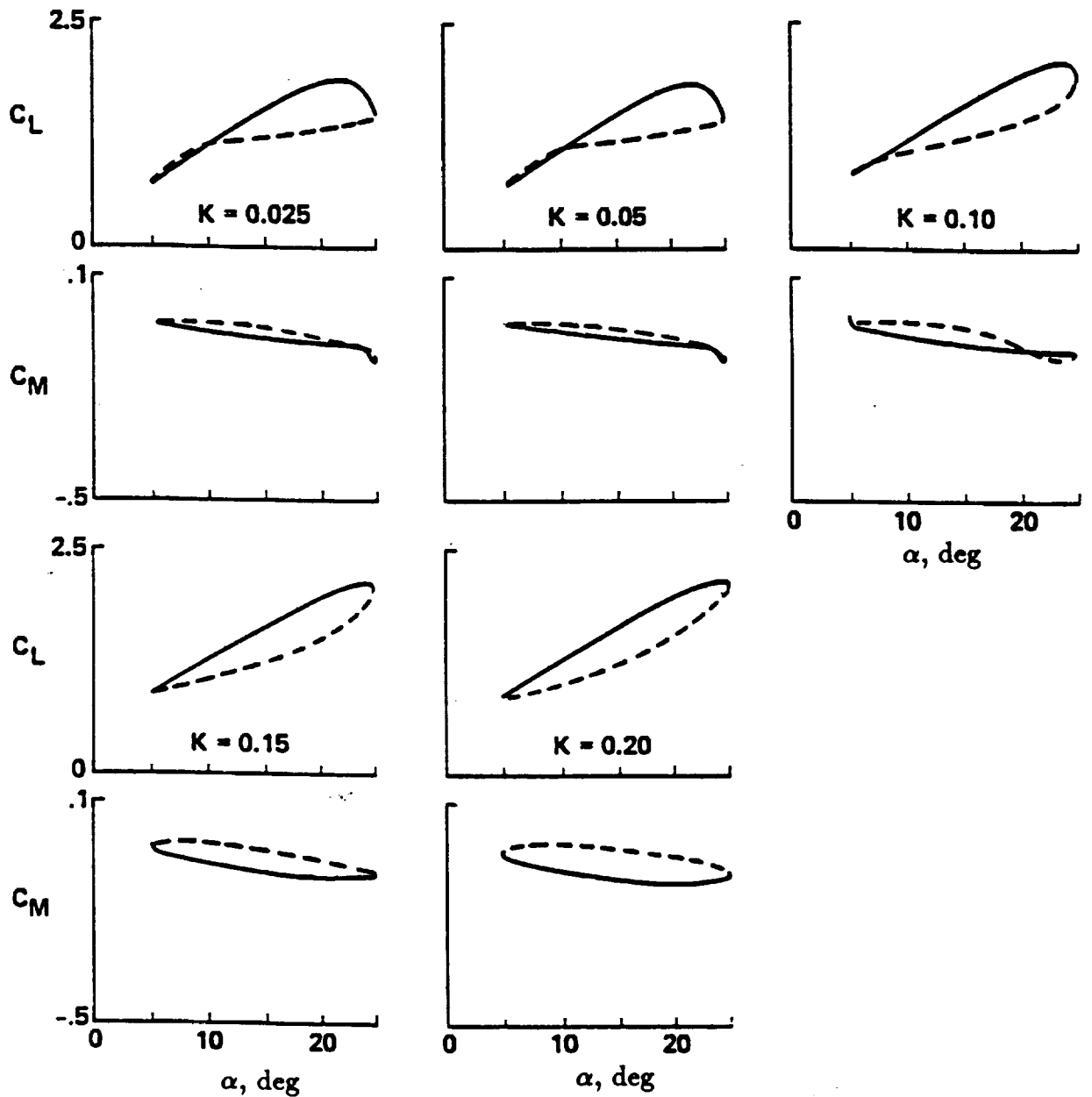


Figure 4.- Lift and moment for the VR-7 airfoil with slat for $\alpha = 15^\circ + 10^\circ \sin \omega t$, $M_\infty = 0.185$, $Re = 2.5 \times 10^6$ and a range of frequencies. Dashed lines indicate decreasing α .

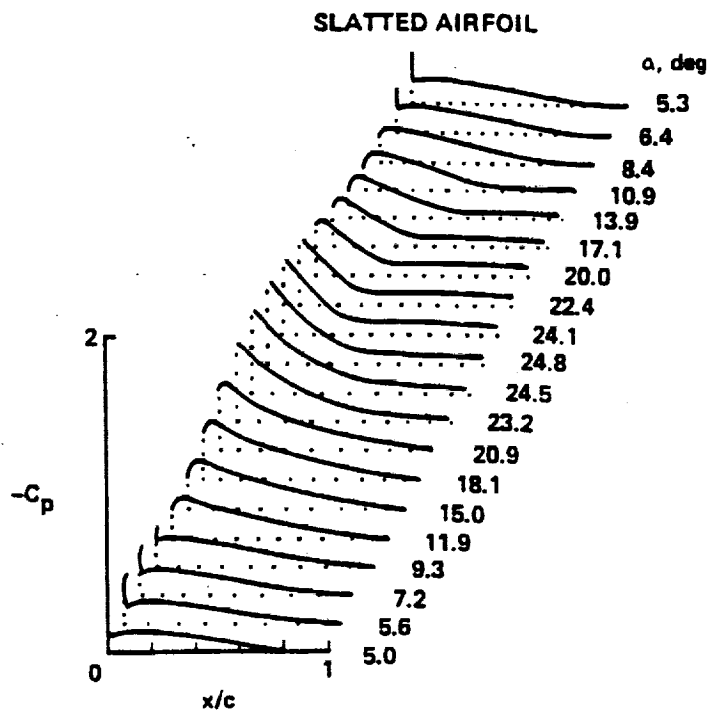
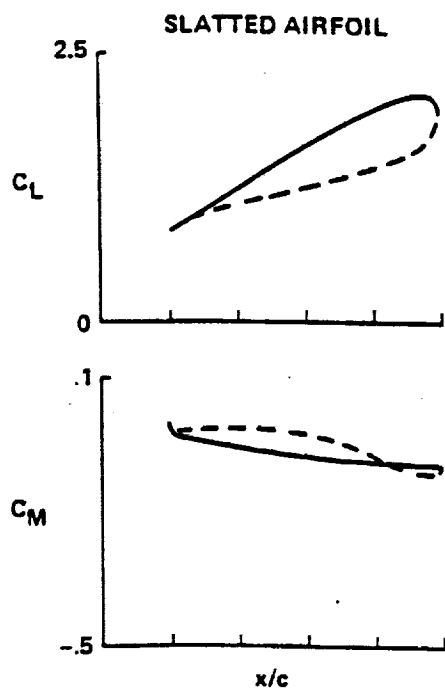
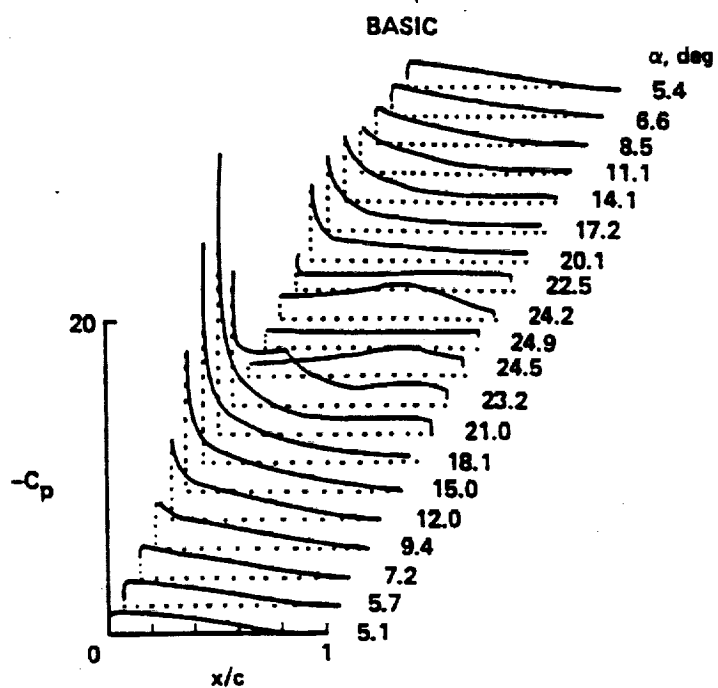
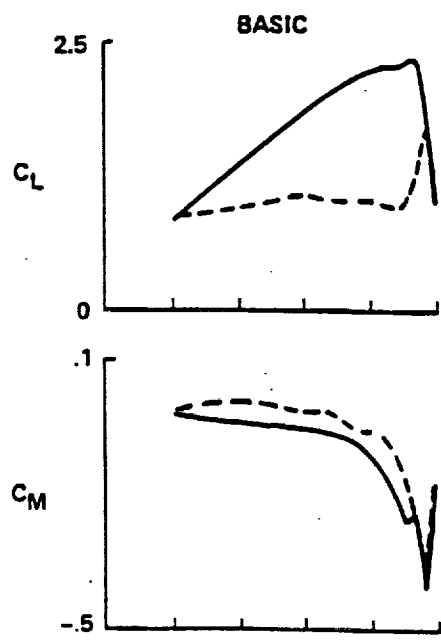
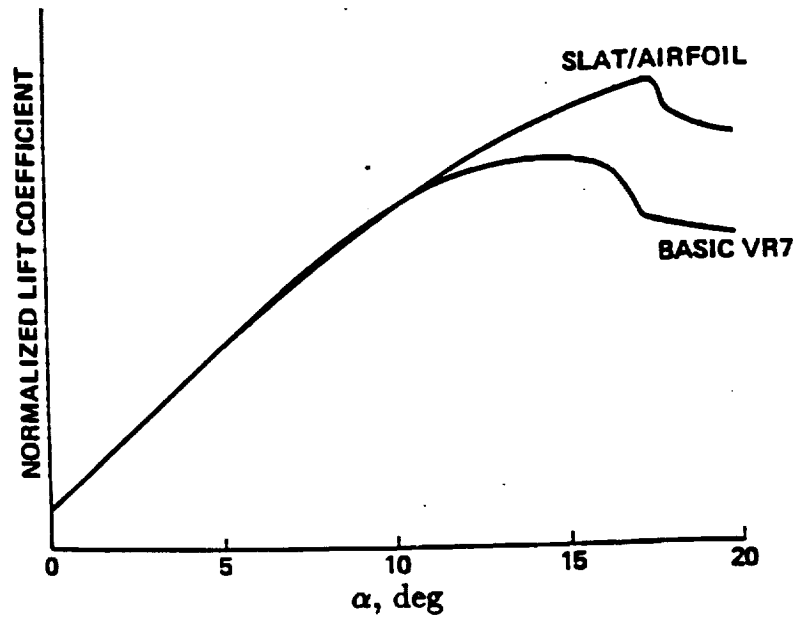
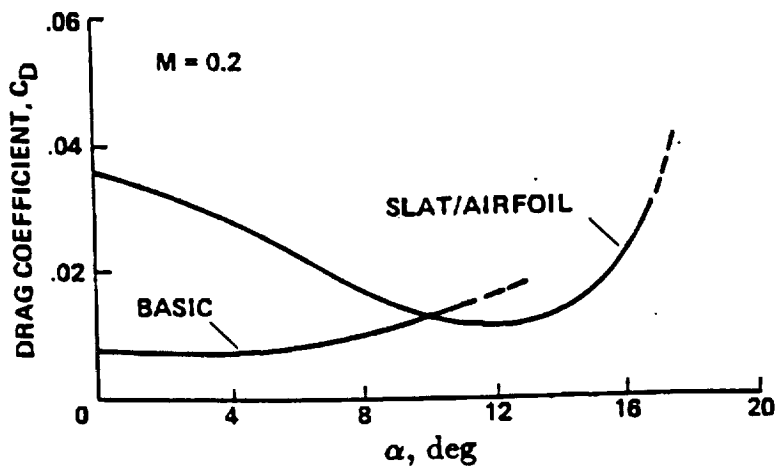


Figure 5.- Lift, moment and pressure for the basic and slatted VR-7 airfoils for $\alpha = 15^\circ + 10^\circ \sin \omega t$, $k = 0.1$, $M_\infty = 0.185$ and $Re = 2.5 \times 10^6$. Dashed lines indicate decreasing α .



(a) Quasi-static lift.



(b) Wake drag.

Figure 6.- Lift and drag measurements for the basic and slatted VR-7 airfoils at $M_\infty = 0.185$ and $Re = 2.5 \times 10^6$.

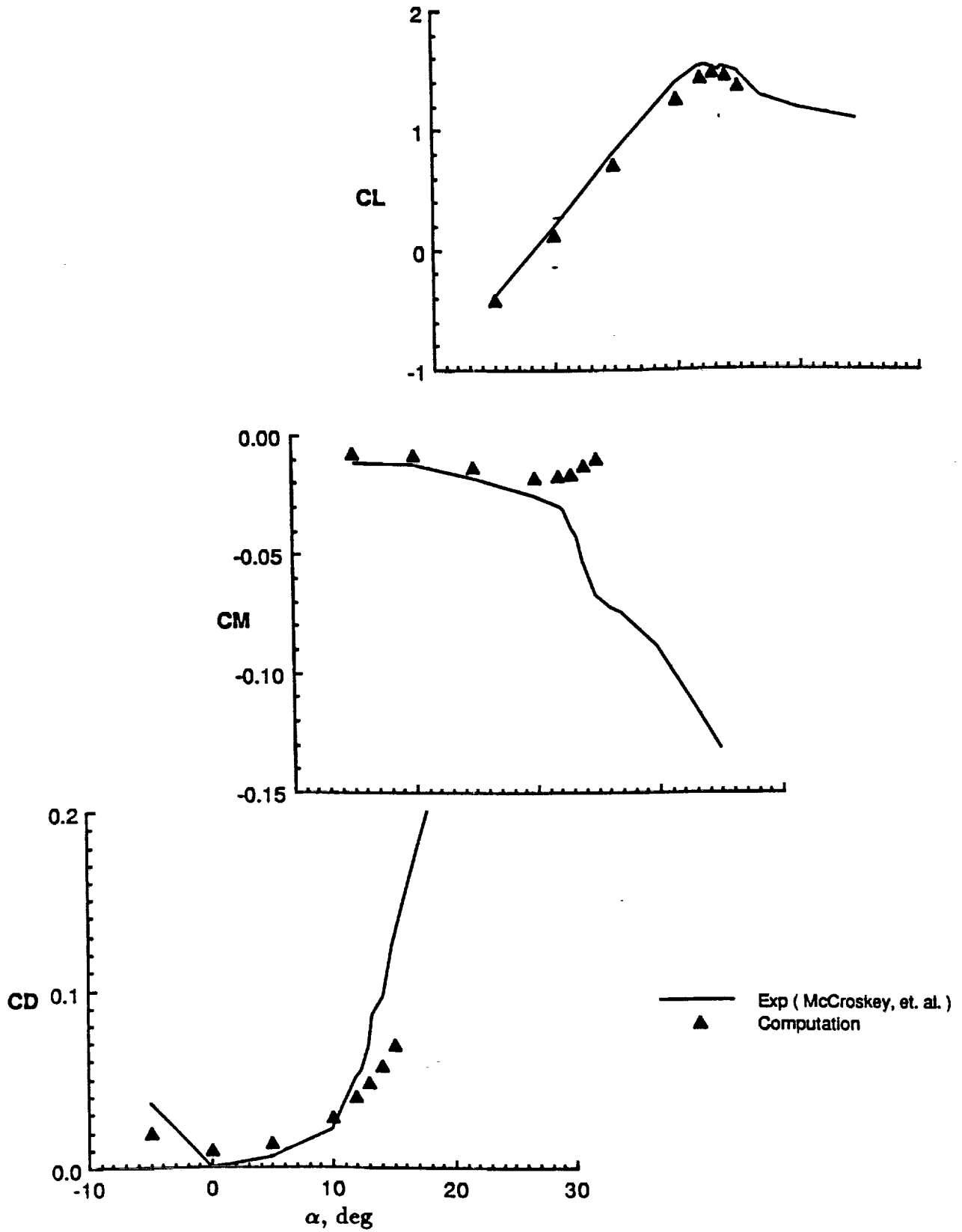


Figure 7.- Force and moment calculations for the basic VR-7 airfoil at $M_\infty = 0.3$ and $Re = 4.2 \times 10^6$.

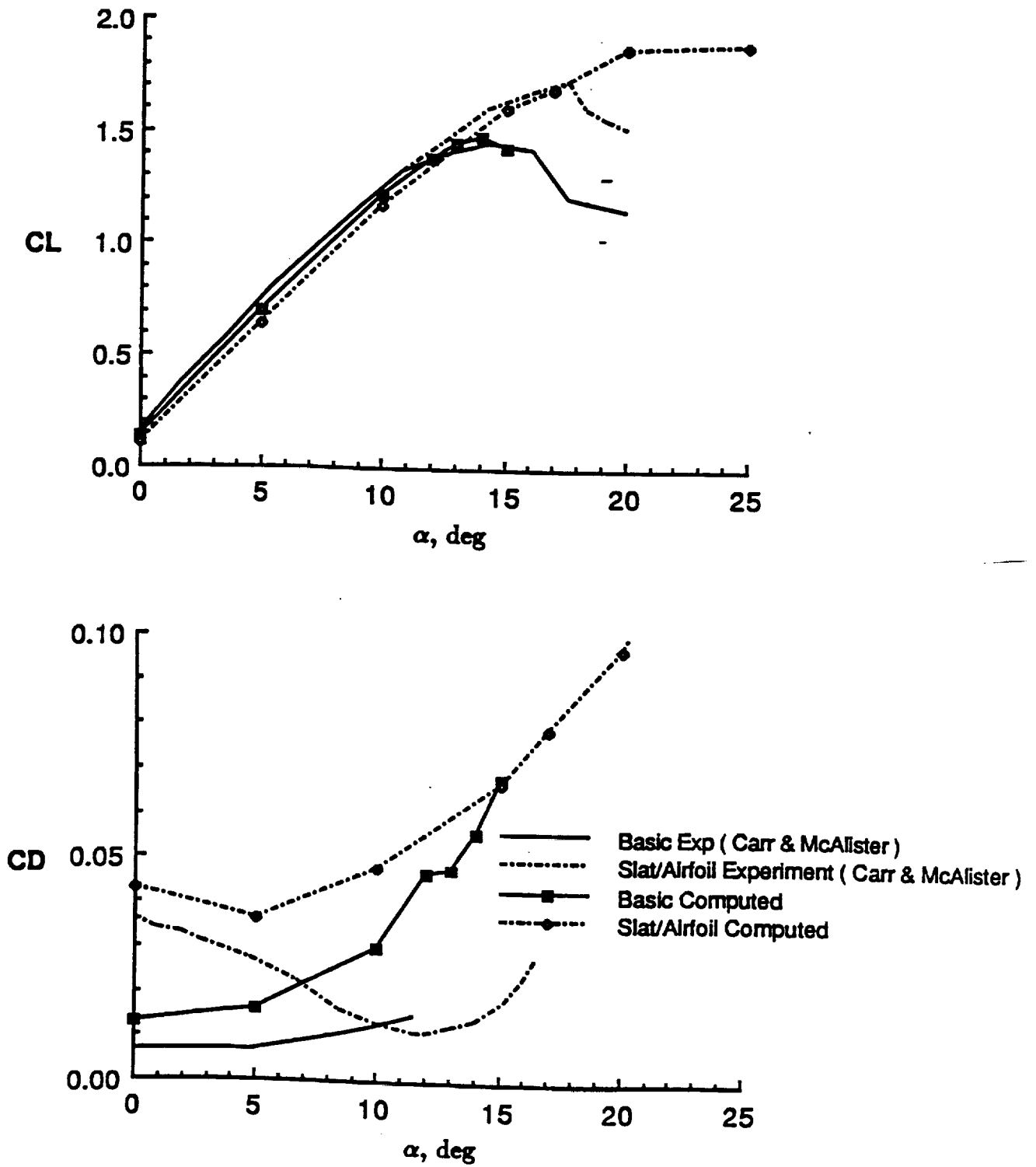
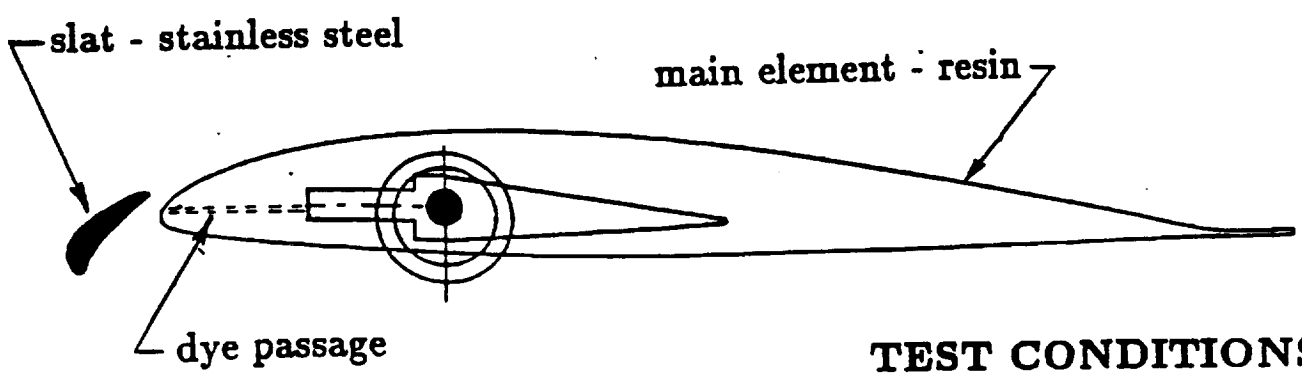
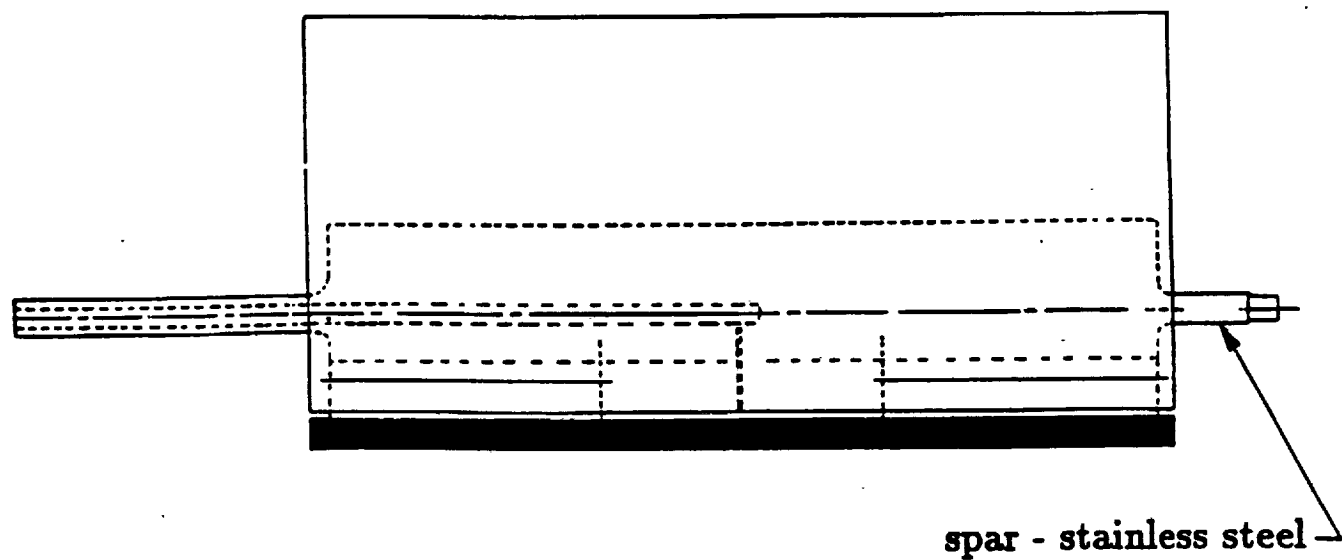
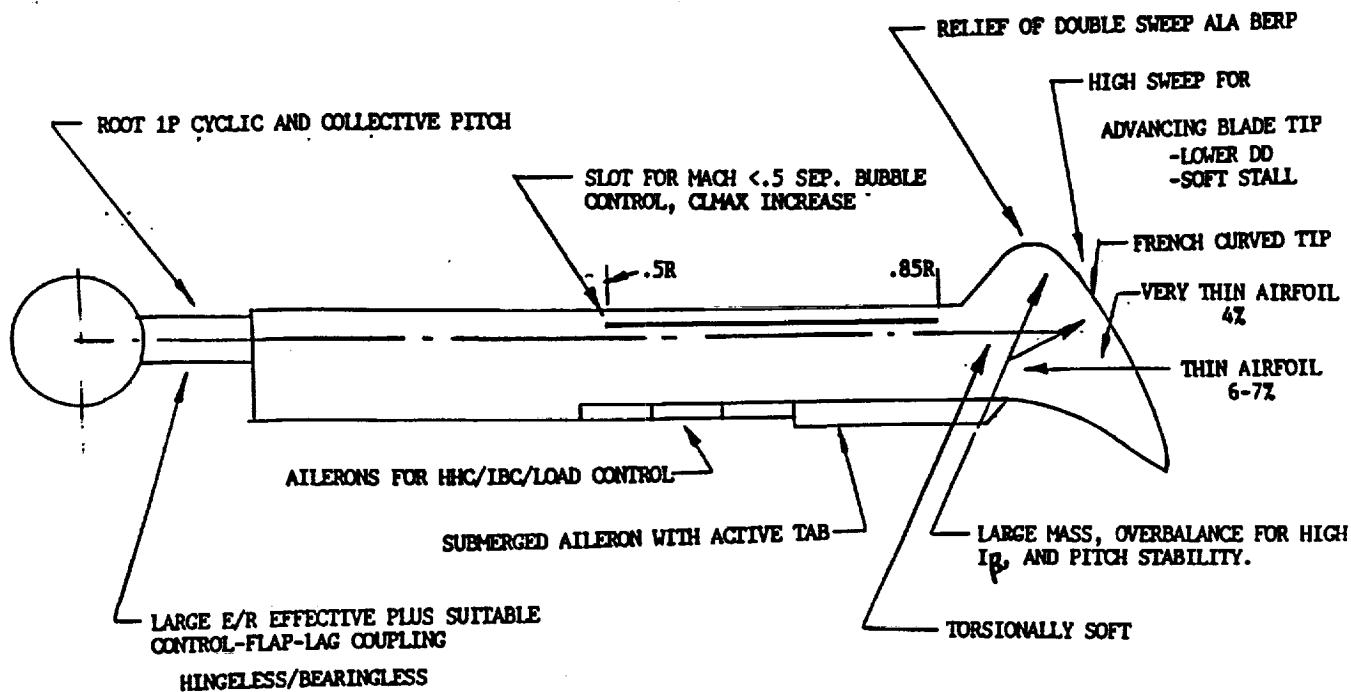


Figure 8.- Lift and drag on the basic and slatted VR-7 airfoils at $M_\infty = 0.185$ and $Re = 2.5 \times 10^6$.



TEST CONDITIONS
 $k = 0.1$
 $Re = 50K \text{ to } 500K$
 $\alpha = \alpha_o + 10 \sin \omega t$

Figure 10.- Water-tunnel model of the VR-7 airfoil with slat.



NON-LINEAR TWIST
-FOR GOOD FM
-REDUCE NEG ANGLE @ 90

HIGH C_{LMAX}
HIGH MAX. LIFT MOMENT @ 270
HIGH LIFT MOMENT/ δ
INTEGRATED FLAP DAMPING

HIMARCS ROTOR
SPECULATIVE PROJECTION

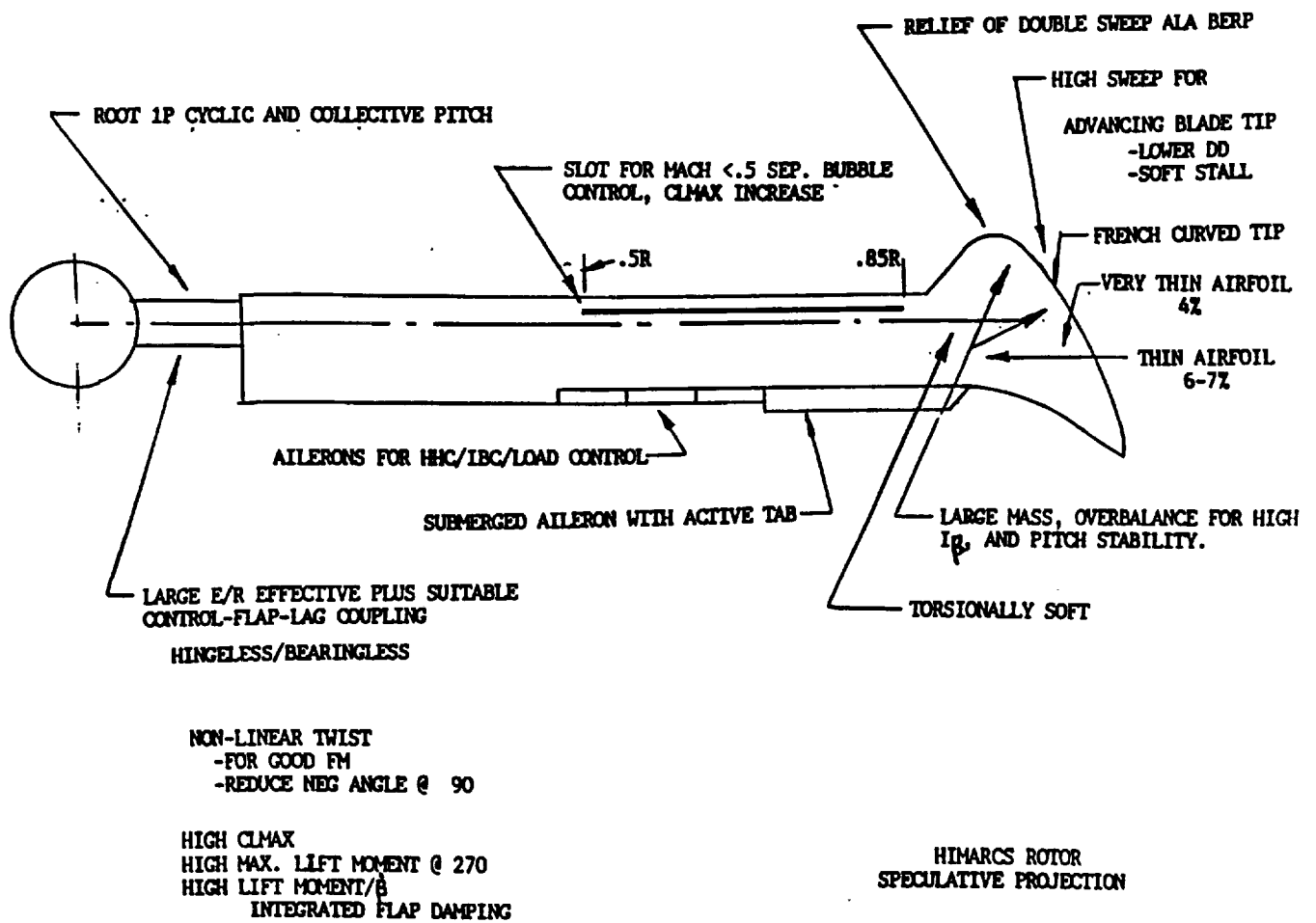


Figure 11.- Wide range of high-lift and control devices considered in HIMARCS.

